Korean Journal of Radiology

KJR

Preoperative Cardiac Computed Tomography Characteristics Associated with Recurrent Aortic Regurgitation after Aortic Valve Re-Implantation

Yura Ahn, MD[1], Hyun Jung Koo, MD, PhD[1], Sahmin Lee, MD, PhD[2], Dae-Hee Kim, MD, PhD[2], Jong-Min Song, MD, PhD[2], Duk-Hyun Kang, MD, PhD[2], Jae-Kwan Song, MD, PhD[2], Ho Jin Kim, MD, PhD[3], Joon Bum Kim, MD, PhD[3], Sung-Ho Jung, MD, PhD[3], Suk Jung Choo, MD, PhD[3], Cheol Hyun Chung, MD, PhD[3], Jae Won Lee, MD, PhD[3], Joon-Won Kang, MD, PhD[1], Dong Hyun Yang, MD, PhD[1]

[1]Department of Radiology and Research Institute of Radiology, Cardiac Imaging Center, [2]Division of Cardiology, and [3]Department of Cardiovascular Surgery, Asan Medical Center, University of Ulsan College of Medicine, Seoul, Korea

Objective: To identify the preoperative cardiac computed tomography (CT) factors influencing postoperative recurrent aortic regurgitation (AR) in patients who underwent aortic valve repair with the re-implantation technique (David operation) due to AR.

Materials and Methods: A total of 117 patients (age, 49.4 ± 15.6 years; 83 males) who underwent the David operation for AR were included in this retrospective study. Aortic root profiles including the aortic regurgitant orifice area (ARO) and the aortic cusp asymmetry ratio of the areas (ASR$_{area}$), which is defined as the maximum/minimum areas among the three cusp areas at the level of the commissures, were measured on preoperative cardiac CT scans. Clinical and CT findings were compared between a group with recurrent AR grade < 3 (no, trivial, or mild AR) and recurrent ≥ 3 + AR. To determine the optimal cut-off values of ASR and ARO, the receiver operating characteristic (ROC) curve was used. Cox regression analysis was used for the analysis of the factors affecting recurrent 3 + AR.

Results: Postoperatively, recurrent 3 + AR developed in 17 (14.5%) patients and occurred within a median of 268 days (interquartile range: 78–582 days). The cut-off ARO value for discriminating the patients with recurrent 3 + AR was > 24 mm^2 (sensitivity, 76.5%; specificity 64.8%), and the area under the ROC curve (AUC) was 0.72. For ASR$_{area}$, the cut-off value was > 1.58 (sensitivity, 76.5%; specificity, 58.0%) and the AUC was 0.64. Multivariable Cox regression showed that ARO > 24 mm^2 (hazard ratio = 3.79, p = 0.020) was a potential independent parameter for recurrent 3 + AR. ROC for the linear regression model showed that the AUC for both ARO and ASR$_{area}$ was 0.73 (95% confidence interval, 0.64–0.81, p < 0.001).

Conclusion: ARO and ASR$_{area}$ detected on preoperative cardiac CT would be potentially helpful for identifying AR patients who may benefit from the David operation.

Keywords: *Aortic valve; Aortic valve insufficiency; Computed tomography angiography; Echocardiography*

INTRODUCTION

Aortic valve replacement (AVR) improves the prognosis in patients with severe aortic regurgitation (AR) (1, 2);

however, the occurrence of prosthesis-related complications cannot be ignored (3). Systemic thromboembolism, valve thrombosis, anticoagulation-induced bleeding, prosthetic valve endocarditis, and structural deterioration of the

prosthetic valves are the risks associated with surgical AVR (4). The cumulative risk of valve-related complications increases up to 50% at 10 years after AVR for the treatment of AR (4, 5).

Aortic valve (AV) repair while maintaining the normal AV architecture is one of surgical options in young adult patients because lifelong anticoagulation and the valve durability after AVR can be problematic in these patients (6-9). Surgical techniques for valve repair are applied according to the function of the leaflets and the size of the aortic root and ascending aorta. Several studies have demonstrated that AV repair is feasible in patients with AR caused by aortic root diseases or aortic cusp prolapses and that the incidence of valve-related complications, including reoperations, was low (6-8, 10-12). In a previous study, AV repair showed improved postoperative patient survival compared to AVR in patients with severe AR (13). The reoperation rate was slightly higher in the AV repair group, but there was no statistical significance (8% vs. 2%, log-rank p = 0.350) (13). Despite these excellent results, it is still uncertain which patients will benefit from AV repair, and the preoperative prognostic factors for recurrent AR and reoperation are unknown.

Cardiac computed tomography (CT) has been used for preoperative AV assessment along with echocardiography, and CT allows detailed anatomical measurements and has shown excellent correlation with surgical findings (14). The shape of the aortic root, including aortic cusp asymmetry and the aortic regurgitant orifice area (ARO), can be easily assessed by CT multiplanar reconstruction images. The purpose of this study is to identify the factors influencing the development of postoperative, recurrent AR and the consequential reoperation using preoperative clinical and cardiac CT findings in patients who underwent AV repair with a re-implantation technique (David operation).

MATERIALS AND METHODS

Patient Population

This retrospective observational study was approved by the Institutional Review Board (approval number: 2018-1189), and the need for written informed consent was waived. In our hospital, AV repair with the re-implantation technique (David operation) is routinely performed for AR. We searched the cardiac surgery registry and medical records at our institution to identify consecutive patients who underwent AV-sparing surgery for AR and preoperative

cardiac CT between January 2011 and April 2019. A total of 139 patients with AR underwent AV-sparing surgery for aortic root enlargement (n = 131), AV prolapse (n = 7), or cusp retraction (n = 1). Twelve patients (4 who underwent CT at other institutions and eight who underwent non-cardiac gated CT) who did not undergo preoperative multiphase cardiac CT were excluded. We also excluded two patients who had type I aortic dissection involving the aortic root because they underwent emergency surgery without electrocardiogram-gated cardiac CT scanning and measurement of the aortic root dimension was limited by motion artifacts of the dissecting intimal flap. In eight patients, AV-sparing operations were intraoperatively converted to Bentall operations due to failure of the David operation. Finally, 117 patients (age, 49.4 ± 15.6 years; 83 males) with preoperative cardiac CT scans were evaluated, and preoperative and postoperative follow-up echocardiography and medical records were thoroughly reviewed. All patients underwent intraoperative transesophageal echocardiography (TEE) and postoperative transthoracic echocardiography two days following surgery. Follow-up transthoracic echocardiography was performed after 6 months and every 6–12 months thereafter.

CT Protocol and Image Analysis

Preoperative cardiac CT was performed using a second generation, dual-source CT scanner (SOMATOM Definition Flash, Siemens Healthineers, Forchheim, Germany). Cardiac scanning was performed using a retrospective electrocardiogram-gated protocol. Detailed CT protocols are included in Supplementary Materials. CT data sets were reconstructed using a 10% R-R interval. Post-processing was performed using an external workstation (AquariusNet, TeraRecon, Foster City, CA, USA). Three diagnostic views were obtained for AV assessment: en-face view; oblique coronal view; and three-chamber view. The en-face view of the AV is parallel to the transverse plane of the three coronary sinuses. The three-chamber view (left ventricular [LV] outflow tract view) and oblique coronal view are perpendicular to each other. The ARO was measured from the en-face view on the end-diastolic phase of the CT images. For evaluation of the ARO using the planimetry method, images with 5–10-mm slice thickness were used to delineate the tips of the aortic cusps (Fig. 1). The aortic cusp asymmetry ratio (ASR) was obtained by determining the ratio of the diameters ($ASR_{diamter}$, the maximum length/ minimum length among the three diameters that connect
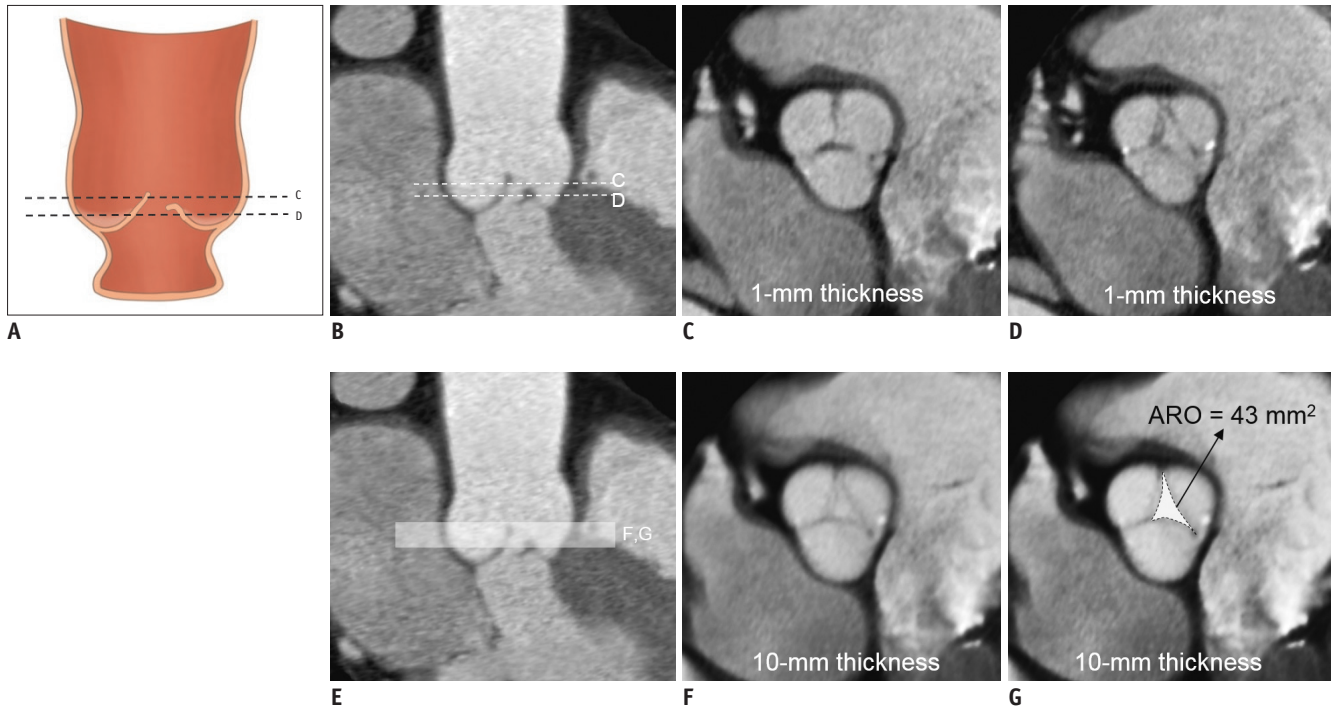
Fig. 1. Measurement of ARO.
A. Schema of AR with prolapse of coronary cusp. **B.** Patient with prolapse of right coronary cusp causing AR. Levels of tips of cusps are not parallel to annulus level. En-face view of AV at level of **C**, dotted line in **(A)** and **(B)**, is depicted in **(C)**, and tip of right coronary cusp is not delineated on this level. At level of **(D)**, right coronary cusp is noted, but ARO cannot be drawn below intercommissural points. **(E)** Using 10-mm thickness images (white box area) in en-face view, we can include tips of coronary cusps as depicted in figure **(F)**, and ARO is drawn (dotted area) **(G)**. All CT images are obtained on end-diastolic phase. AR = aortic regurgitation, ARO = aortic regurgitant orifice area, AV = aortic valve

one commissure to the tip of the opposite cusp) or areas (ASR$_{area}$, the maximum size of the cusp to the minimum size of the cusp), and this was measured from the en-face view of the AV on the end-systolic phase and at the level at which the cusps sizes are maximal (Fig. 2). We chose the end-systolic phase because when aortic cusp prolapse occurred during diastole, the prolapsed leaflet margin could not be drawn in the same image plane with other normal leaflets. In patients with a bicuspid valve with raphe, the locations of aortic cusps were designated as the tricuspid valve. In bicuspid valves without raphe, ASR was calculated using the two cusps. The aortic root parameters were evaluated in consensus by two radiologists who were blinded to the clinical information, echocardiography findings, and surgical records. ARO and ASR were independently measured by a third radiologist to determine interobserver reliability.

Echocardiography

Echocardiography was performed using one of two commercial ultrasound machines with 3–5 MHz real-time transducers (Sonos 7500, Philips Medical Systems, Andover, MA, USA; Vivid 7, GE Healthcare, Waukesha, WI, USA). Expert cardiologists obtained preoperative, conventional, two-dimensional and Doppler images, and the images were stored digitally. Color Doppler images were obtained for evaluation of AR. The AR severity was graded over four degrees using the color Doppler grading system introduced by Perry et al. (15) with the jet height/LV height. Other parameters, including the LV ejection fraction and volumetric parameters such as the LV end-systolic volume index (ESVI), end-diastolic volume index (EDVI), and internal dimensions, were reviewed.

Functional Classification of AR

The aortic root and cusps were classified into three groups according to previously established surgical criteria: type 1, ascending aorta or aortic sinus or root dilatation exceeding the normal limits (16) (sinus, 45.4 mm; sinotubular junction [STJ], 37.8 mm; and mid-ascending aorta, 42.5 mm) with a normal cusp or perforation of the cusp (Supplementary Fig. 1): type 1a resulting from STJ and ascending aorta dilatation, type 1b resulting from dilatation of the sinus of Valsalva and STJ, type 1c resulting from dilatation of
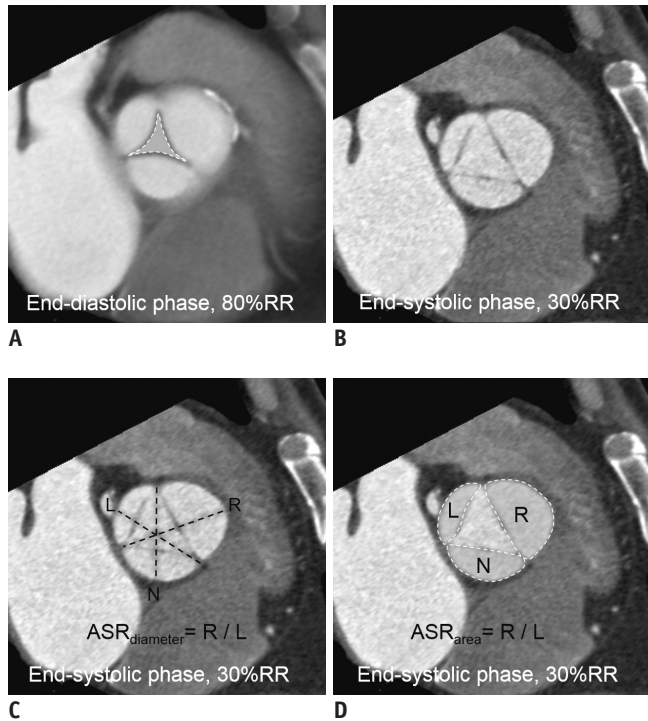
Fig. 2. Measurement of aortic cusp ASR.
A. Measurement of ARO (dashed white line) on AV en-face view when in end-diastolic phase. Cross-sectional image is acquired with 10-mm thick-slab overlapping. **B.** AV en-face view when in end-systolic phase at level comprising all three commissures. **C.** $ASR_{diameter}$ was defined as maximum/minimum lengths among three diameters (dashed lines) from one commissure to tip of opposite cusp. **D.** ASR_{area} was defined as maximum/minimum areas among three cusp areas (dashed white lines). ASR = asymmetry ratio, ASR_{area} = aortic cusp asymmetry ratio of areas, $ASR_{diameter}$ = aortic cusp asymmetry ratio of diameters, L = left coronary cusp, N = non-coronary cusp, R = right coronary cusp, RR = RR interval

the ventriculoaortic junction, and type 1d resulting from cusp perforation. Type 2 involves cusp prolapse when one or more cusps drop inferiorly to the plane of the aortic annulus. Type 3 involves retraction with thickening of the cusps. Echocardiography or CT results were provided to the surgeons/pathologists before they performed an operation or pathologic specimen evaluation.

Operation Technique

The AV repair was performed using the re-implantation technique (David operation) (17, 18). Briefly, after institution of cardiopulmonary bypass (CPB) and aortic cross-clamping, the aortic root was transected approximately 5 mm distal to the STJ. The left and right coronary arteries were detached as buttons from the dilated aortic sinuses with a small rim of tissue surrounding their orifice for the graft reattachment. The base of the aortic root was dissected down to the level of the nadir of each

of the aortic leaflets for placement of the basal first-line sutures. In preparation for the second-line hemostatic sutures, the aortic root was dissected along the scalloping contour of each of the individual sinuses. A straight dacron tube graft or a Valsalva graft (Vascutek Ltd, Leeds, UK) of appropriate size was selected for re-implantation. Usually, six anchoring first-line sutures were placed with pledgetted multifilament sutures along the plane of the cuspal nadirs. The rim of contiguous tissue adjacent to the valve leaflets was then sutured onto the graft for re-implantation. For cases showing absolute or relative leaflet prolapse as determined by measurement of the leaflet height, the free margin was plicated as necessary to achieve a leaflet height of at least 8–10 mm. When the patients showed concerning leaflet fenestrations, leaflet resuspension was performed. Finally, the resected coronary ostia buttons were re-implanted.

Statistical Analysis

Continuous data are expressed as means ± standard deviations and categorical data as numbers and percentages. Comparisons between a group with recurrent AR grade < 3 (residual 1 + to 2 + AR and no or trivial AR) and the others with recurrent ≥ 3 + AR or redo-David operation were performed using chi-square and Fisher's exact tests for categorical variables and the Student's t test and Mann-Whitney U test for continuous variables. Interobserver agreement values for measurement of ASR and ARO were obtained using two-way random model intra-class correlation coefficient (ICC) analyses with consistency assumption. To determine the optimal cut-off values of ASR and ARO, the receiver operating characteristic (ROC) curve was used. Based on the cut-off values, the ARO and ASR were converted to a binary variable indicating whether the ratio was larger or smaller than the cut-off value. Univariate and multivariable Cox regression analyses were used to assess the relationship between clinical/imaging factors and recurrent AR. Variables with p values < 0.1 in univariate Cox regression analysis were entered into a multivariable Cox regression model. ROC curve analysis was performed for the validation of the multivariable regression model. The Kaplan–Meier method was used to plot the time-to-event curves of the two groups. Statistical analysis was performed using commercial software (SPSS, version 21.0, IBM Corp., Armonk, NY, USA). A p value < 0.05 was considered statistically significant.

Table 1. Comparisons of Patients with Recurrent AR Grade < 3 (No, Trivial, or Mild AR) and Others with Recurrent AR Grade ≥ 3 after AV Repair with Re-Implantation Technique (David Operation)

Recurrent AR	Grade < 3 (n = 100)	Grade ≥ 3 (n = 17)	P
Age, year	49.6 ± 16.1	48.4 ± 13.2	0.781
Male sex	72 (72.0)	11 (64.7)	0.570
Body mass index, m/kg^2	23.7 ± 3.7	22.4 ± 2.4	0.063
Body surface area, m^2	1.8 ± 0.2	1.8 ± 0.2	0.201
B-type natriuretic peptide, pg/mL	34.5 (16.7–103.2)	68.5 (14.2–159.0)	0.513
Echocardiography			
ESVI	60.5 (49.0–92.2)	109.0 (64.0–146.0)	0.004
EDVI	156.5 (124.5–217.0)	236.0 (177.2–316.2)	0.001
LVEF, %	60.0 (57.0–63.2)	58.0 (48.0–65.0)	0.405
Bicuspid AV	7 (7.0)	2 (11.8)	0.617
Functional classification of AR			0.774
Type 1a	44 (44.0)	10 (58.8)	
Type 1b	47 (47.0)	6 (35.3)	
Type 1c	2 (2.0)	0 (0.0)	
Type 2	6 (6.0)	1 (5.9)	
Type 3	1 (1.0)	0 (0.0)	
Marfan syndrome	34 (34.0)	2 (11.8)	0.066
Redo-AV replacement	0 (0.0)	2 (11.8)	< 0.001
Postoperative echocardiography			
ESVI	45.5 (37.7–60.2)	71.5 (42.0–94.2)	0.010
EDVI	118.0 (98.0–137.5)	160.5 (113.0–210.2)	0.002
LVEF, %	59.0 (56.0–63.0)	59.0 (55.2–63.0)	0.991
AR ≥ grade 3	0 (0)	17 (100)	< 0.001
Cardiac CT to operation date, day	21.0 (2.3–54.3)	6.0 (3.0–30.5)	0.538
CT parameters			
ARO, mm^2	16.0 (2.8–32.8)	32.5 (18.3–60.5)	0.003
Annulus			
Maximum diameter, mm	31.0 (29.0–33.0)	32.0 (29.2–33.7)	0.368
Minimum diameter, mm	26.0 (24.0–28.0)	26.0 (23.6–27.8)	0.716
Perimeter, mm	90.0 (85.8–96.5)	92.9 (87.2–98.5)	0.384
Area, mm^2	634.4 (556.6–703.5)	661.8 (563.9–737.5)	0.536
Sinus of Valsalva, mm	55.0 (49.0–60.0)	56.5 (52.3–63.3)	0.526
STJ, mm	49.0 (40.0–58.3)	51.0 (43.0–63.0)	0.432
Ascending aorta tubular portion, mm	40.8 (34.0–47.0)	42.2 (33.7–51.1)	0.315
Retraction of cusps	13 (13.0)	2 (11.8)	1.000
Prolapse of cusps	17 (17.0)	4 (23.5)	0.504
ASR$_{diameter}$	1.1 (1.0–1.1)	1.1 (1.0–1.1)	0.506
ASR$_{area}$	1.5 (1.3–1.8)	1.7 (1.5–1.8)	0.077
Binary, ARO > 24 mm^2	36 (36.0)	13 (76.5)	0.003
Binary, ASR$_{area}$ > 1.58	42 (42.0)	13 (76.5)	0.008
Radiation dose			
mAs	246.6 ± 80.9	264.6 ± 86.0	0.428
Dose length product	1124.5 ± 655.9	1363.8 ± 792.5	0.180

Data are noted as mean and standard deviation, median and interquartile ranges or numbers and percentages in parenthesis. AR = aortic regurgitation, ARO = aortic regurgitation orifice, ASR = aortic cusp asymmetry ratio, ASR$_{area}$ = aortic cusp asymmetry ratio of areas, ASR$_{diameter}$ = aortic cusp asymmetry ratio of diameters, AV = aortic valve, EDVI = end-diastolic volume index, ESVI = end-systolic volume index, LVEF = left ventricular ejection fraction, mAs = miliampere-second, STJ = sinotubular junction

RESULTS

Patients and Operative Outcomes

Baseline characteristics of the 117 patients are shown in Table 1. Nine patients had bicuspid AV (with raphe, 6; without raphe, 3). On CT, the sizes of the cusps at the aortic sinus level were asymmetrically different, and the left coronary cusp was the smallest in 66 (56.4%) patients. In 29 (29.9%) patients, the non-coronary cusp was the smallest, and the right coronary cusp was the smallest in 16 (13.6%) patients.

Operations were performed by 4 of 6 experienced cardiac surgeons. In conjunction with ascending aorta replacement, total arch and hemiarch replacement were performed in 17 (14.5%) patients and 27 (23.1%) patients, respectively, and in 5 (4.3%) patients, only ascending aorta replacement was performed. Ascending aorta wrapping was performed in 5 (4.3%) patients. Concomitant coronary artery bypass was performed in 3 (2.6%) patients. All patients underwent intraoperative TEE after CPB weaning. CPB was re-applied in five patients for revision due to immediate postoperative AR detected on intraoperative TEE. The five patients showed no or trivial AR after the revision, and one of the patients developed recurrent AR two years after the David operation.

After a median follow-up duration of 16.2 months (interquartile range, 3.4–31.2 months), 17 (14.5%) patients had recurrent ≥ 3 + AR (Fig. 3), 52 patients presented with residual 1 + to 2 + AR, and 48 had no or trivial AR. The median interval between the David operation and the date of the recurrent AR detection was 268 days (interquartile range: 78–582 days). The 3-year recurrent AR-free survival rate was 76.3%. Among the 17 patients with recurrent ≥ 3 + AR, two underwent reoperation on the re-implanted aortic root. One patient with grade 4 AR underwent AVR, and the other patient underwent redo-David operation for grade 3 AR with recurrent annuloectasia.

AR Classification on Echocardiography and CT

On surgical inspection for patients who underwent the David operation, type 1a AR was the most common (n = 54), followed by type 1b (n = 53), type 2 (n = 7), type 1c (n = 2), and type 3 (n = 1) (Table 2). Cohen's kappa for agreement of the CT and echocardiographic findings with the results of surgical inspection as the reference standard was 0.85 for CT and 0.95 for echocardiography.

Prediction of Recurrent 3 + AR after David Operation

Intra-observer agreement for ARO and ASR_{area} were excellent (ICC = 0.99 for both). Patients with ARO > 24 mm^2 (36.0 vs. 76.5%, p = 0.003) or ASR_{area} > 1.58 (42.0 vs. 76.5%, p = 0.008) were significantly more common in the recurrent 3 + AR group. On ROC analysis, the cut-off value for predicting postoperative recurrent 3 + AR was 24 mm^2 (sensitivity, 76.5%; specificity, 64.8%), and the area under the ROC curve (AUC) was 0.72 (95% confidence interval
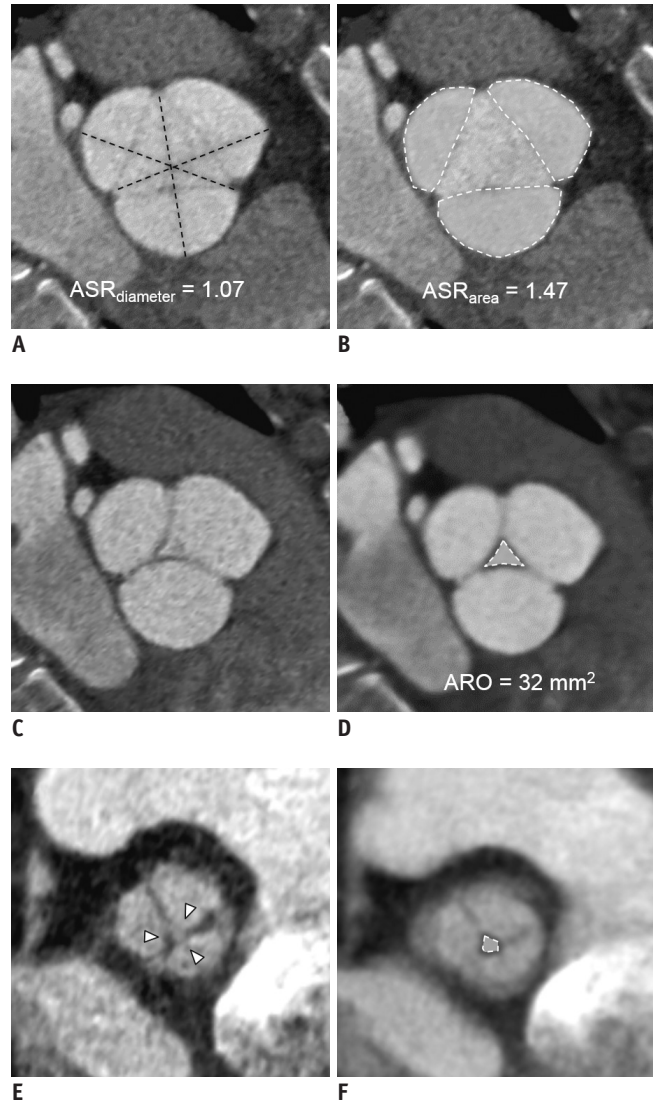

Fig. 3. 34-year-old female with type 1a AR.
A, B. Aortic cusp $ASR_{diameter}$ (dashed lines) and ASR_{area} (dashed white lines) were measured on end-systolic phase. **C, D.** ARO was measured on end-diastolic phase. **(C)** Leaflets are not well demonstrable on 1-mm thickness image of AV in en-face view; therefore, **(D)** 5–10-mm-thick slices are used to measure ARO (dashed white line). **E.** On postoperative CT, four days after David operation, AV en-face view on end-diastolic phase demonstrated small central coaptation defect (arrowheads). **F.** Recurrent ARO was noted on thick-slice thickness (dotted-lined area). On same day, grade 3 AR was detected.

https://doi.org/10.3348/kjr.2019.0446

Table 2. Agreement of AR Classification on CT and Echocardiography with Findings of Surgical Inspection

Findings	Surgical Inspection, n					Total
	Type 1a	Type 1b	Type 1c	Type 2	Type 3	
CT						
Type 1a	48	4	0	0	0	52
Type 1b	5	49	0	0	0	54
Type 1c	0	0	2	0	0	2
Type 2	1	0	0	7	0	8
Type 3	0	0	0	0	1	1
Total	54	53	2	7	1	117
Echocardiography						
Type 1a	52	1	0	0	0	53
Type 1b	2	52	0	0	0	54
Type 1c	0	0	2	0	0	2
Type 2	0	0	0	7	0	7
Type 3	0	0	0	0	1	1
Total	54	53	2	7	1	117

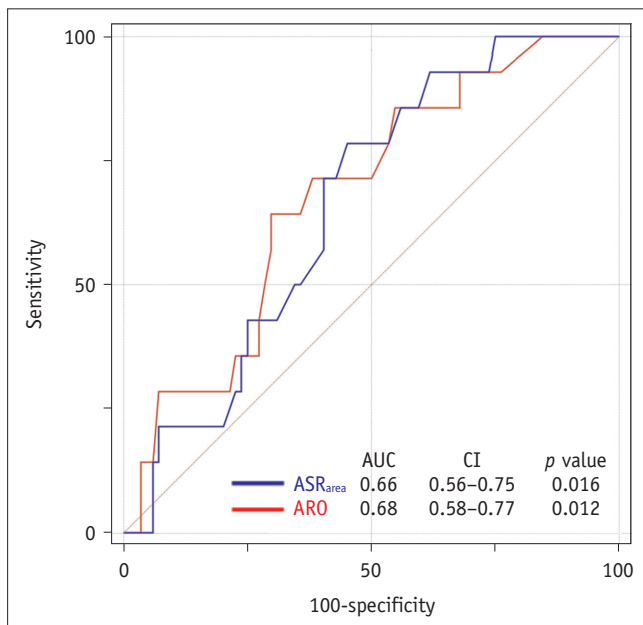|	AUC	CI	p value
ASR$_{area}$	0.66	0.56–0.75	0.016
ARO	0.68	0.58–0.77	0.012

Fig. 4. ROC curves for two cardiac CT predictive factors (ARO and aortic cusp ASR$_{area}$) for predicting recurrent 3 + AR after AV repair with re-implantation technique (David operation). AUC = area under ROC curve, CI = confidence interval, ROC = receiver operating characteristic

[CI] 0.63–0.80, $p < 0.001$) (Fig. 4). The cut-off ASR$_{area}$ value for predicting postoperative recurrent 3 + AR was 1.58 (sensitivity, 76.5%; specificity, 58.0%), and the AUC was 0.64 (95% CI 0.54–0.72, $p = 0.04$). In case of ASR$_{diameter}$, the cut-off value for predicting postoperative recurrent 3 + AR was 1.07 (sensitivity 58.8%, specificity 61.0%), and the AUC was 0.55 (95% CI 0.39–0.71, $p = 0.51$). Therefore, we chose the ASR$_{area}$ instead of the ASR$_{diameter}$ as the parameter for binary conversion. The ROC for the linear regression

model using both ARO and ASR$_{area}$ showed that the AUC for both ARO and ASR$_{area}$ was 0.73 (95% CI, 0.64–0.81, $p < 0.001$), and there were no statistical differences between the three ROC curves ($p > 0.05$).

On univariate Cox regression analysis, ARO > 24 mm^2, ASR$_{area}$ > 1.58, ESVI, and EDVI on preoperative echocardiography were significant predictive factors for recurrent 3 + AR ($p < 0.05$ for all comparisons) (Table 3). In the multivariable Cox regression model, ARO > 24 mm^2 was independently associated with recurrent 3 + AR (hazard ratio [HR], 3.79; 95% CI, 1.23–11.70; $p = 0.020$). ASR$_{area}$ > 1.58 was not a statistically significant factor (HR, 2.72; 95% CI, 0.88–8.39; $p = 0.085$). The presence of a bicuspid valve itself was not a significant factor associated with postoperative recurrent 3 + AR. Cox analysis results after excluding nine patients with bicuspid valve are included in Supplementary Table 1, but the results are similar to the original result that included bicuspid valves.

The Kaplan–Meier analysis showed the time to the development of recurrent 3 + AR (Fig. 5). Recurrent 3 + AR was more common in patients who had ARO > 24 mm^2 or ASR$_{area}$ > 1.58 than in those who did not. The difference between the curves was significant with an ARO cut-off value of 24 mm^2 (log-rank test, $p = 0.005$). Curves with an ASR$_{area}$ cut-off value of 1.58 also showed a significant difference (log-rank test, $p = 0.032$).

DISCUSSION

In this study, we showed that the ARO and ASR$_{area}$ measured on preoperative CT images were associated with

Table 3. Univariate and Multivariable Cox Regression Analyses to Identify Clinical and CT Predictors of Postoperative Recurrent 3 + AR after AV Repair with Re-Implantation Technique (David Operation)

Variables	Univariable			Multivariable		
	HR	95% CI	P	HR	95% CI	P
Age	1.00	0.96–1.03	0.994			
Male sex	1.35	0.50–3.67	0.554			
Body mass index, m/kg^2	0.92	0.81–1.05	0.236			
Body surface area, m^2	0.27	0.24–2.94	0.277			
B-type natriuretic peptide, pg/mL	0.99	0.99–1.00	0.515			
Echocardiography						
ESVI	1.01	1.00–1.02	0.002			
EDVI	1.01	1.00–1.01	0.001			
LVEF	0.96	0.90–1.02	0.088			
AR classification						
Type 1a	1.00		0.962			
Type 1b	0.74	0.09–5.98	0.774			
Type 1c	0.77	0.28–2.13	0.965			
Type 2 or 3	0.00	0.00–0.00	0.986			
Bicuspid AV	1.48	0.33–6.63	0.719			
ARO*/10 mm^2	1.26	1.05–1.51	0.015			
Binary ARO > 24 mm^2	4.26	1.38–13.09	0.005	3.79	1.23–11.70	0.020
Annulus maximum diameter, mm	1.06	0.95–1.18	0.295			
Annulus minimum diameter, mm	1.05	0.93–1.21	0.416			
Annulus perimeter, mm	0.99	0.96–1.03	0.556			
Annulus area, mm^2	1.00	0.99–1.00	0.631			
Sinus of Valsalva diameter, mm	1.01	0.96–1.06	0.705			
STJ diameter, mm	1.00	0.96–1.04	0.897			
Ascending aorta tubular portion diameter, mm	1.02	0.97–1.08	0.384			
Retraction of cusps	1.06	0.24–4.63	0.941			
Prolapse of cusps	1.14	0.36–3.58	0.819			
ASR$_{diameter}$	5.99	0.08–465.45	0.426			
ASR$_{area}$	1.16	0.61–2.20	0.731			
Binary, ASR$_{area}$ > 1.58	3.18	1.04–9.74	0.044	2.72	0.88–8.39	0.085

Variables with p values less than 0.1 in univariate Cox regression analysis were entered into multivariable Cox regression model with backward elimination method. *HR for ARO is obtained per 10 mm^2. CI = confidence interval, HR = hazard ratio

recurrent AR after the David operation. ARO > 24 mm^2 was identified as an independent predictor of recurrent 3 + AR. Asymmetric aortic cusps are prone to develop recurrent AR after the David operation, and the cut-off ASR$_{area}$ value was 1.58.

The David operation is a well-established technique in AR and can help eliminate anticoagulation-related problems and the resultant thromboembolic events. The main concern after this operation is recurrent AR (17). Previous studies have revealed predictive factors based mainly on intra- or postoperative echocardiography findings such as the level or length of coaptation, annulus size, and residual AR immediately following the surgery (19, 20). Alternatively,

cardiac CT is currently the emerging imaging modality as it can assess the aortic cusps and root in detail and simultaneously evaluate the coronary artery. As predictors of postoperative recurrent 3 + AR, the preoperative cardiac CT parameters ASR$_{area}$ and ARO, could help identify patients who may benefit from the David operation rather than AVR and vice versa. Further studies with large cohorts to identify whether the CT findings can potentially be used as predictive factors for the failure of the David operation are needed.

The plane of the STJ and the plane at the basal attachment of the aortic annulus are usually nonparallel, and the individual aortic sinuses and cusps are asymmetrical
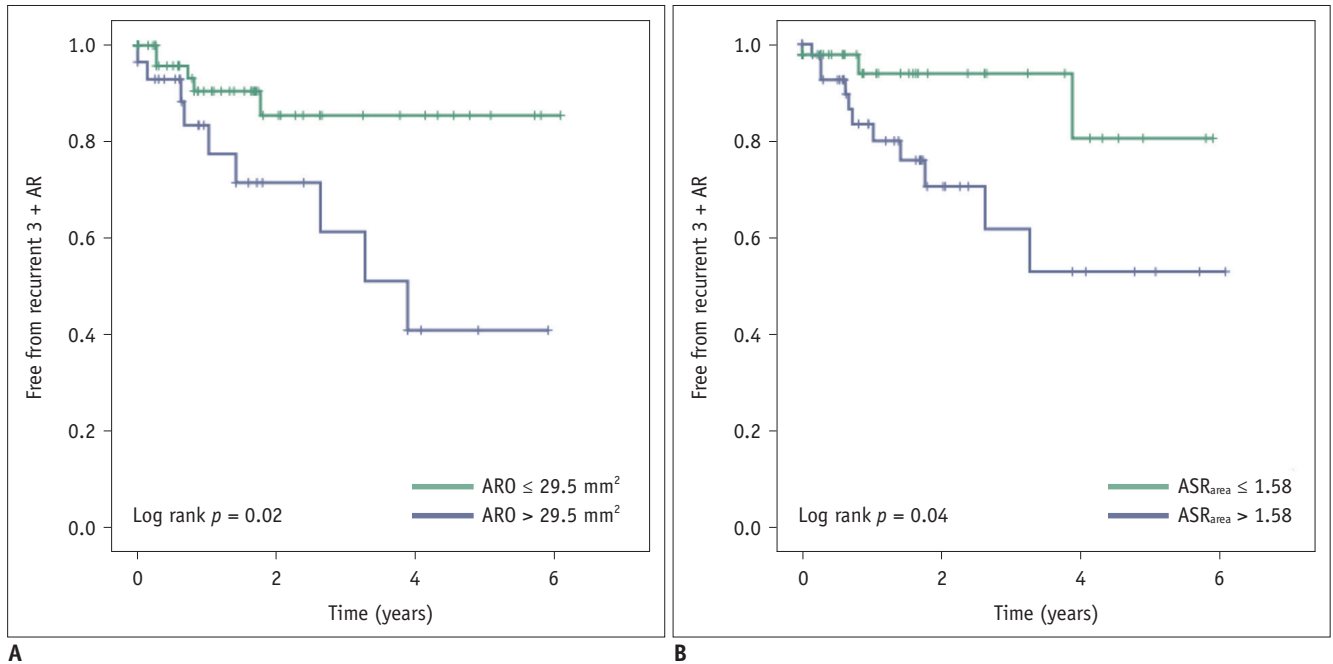
Fig. 5. Kaplan–Meier survival analysis of curves for absence of recurrent 3 + AR according to preoperative cardiac CT parameters (ARO [A] and aortic cusp ASR_{area} [B], respectively).

with respect to one another (21, 22). While cusp asymmetry is often accentuated with root dilatation in AR, aortic cusp enlargement occurs through various hemodynamic influences on cusp adaptation and distensibility (23). The aortic root is a three-dimensional structure in which the individual cusps, sinuses, and the annulus coexist in a spatial geometric relationship that is defined by the variability in their respective depths, widths, and heights. Due to this normally existent complex geometry, the ability of the surgeon to restore the root to its native configuration is extremely limited. As the aortic root dilates, it becomes more asymmetric and when the ability to adaptation of cusps is limited, AR occurs (23). Because AV repair is a procedure that generates an ideal diameter of graft symmetrically including the three cusps, we thought that aortic cusp asymmetry could be a possible factor influencing the level of difficulty of operation and is consequently related to remnant AR. The greater the pre-existent native asymmetry, the greater will be the tendency for the root to deviate from its native asymmetrical state secondary to the inherent tendency of the surgical repair to induce a structurally symmetrical root postoperatively. A previous study reported the association of the aortic symmetric index on TEE with recurrent AR after AV-sparing surgery (24). The resultant geometric distortions, albeit inadvertent, may ultimately contribute to the development

of recurrent AR, and it is our contention that the ASR_{area} observed in our study is a reflection of these geometric alterations resulting thereof.

Our study has several limitations. First, we retrospectively included patients who underwent the David operation and preoperative cardiac CT. Patients who had not undergone preoperative cardiac CT were excluded. However, in our hospital, we routinely performed preoperative cardiac CT before the David operation, except in individuals who have contraindications for a CT exam. Second, although we thoroughly evaluated CT findings to describe the mechanism of AR, structural CT images could not reflect hemodynamic information. Vice versa, the mechanism of AR may not be detectable by surgical inspection of a non-physiological, flaccid heart during open-heart surgery. However, preoperative cardiac CT with multiphase data can provide information regarding the exact motion of aortic leaflets as well as morphological information regarding the aortic root that may associated with the repairability of AR. Preoperative cardiac CT-driven ARO and ASR_{area} assessments may help decision-making when choosing the operation type and considering conversion to AV replacement during the operation. Third, the binary values of ARO and ASR_{area} were used because of the small number of patients. Further studies to confirm the effectiveness of ARO and ASR_{area} for predicting AV repairability are warranted. Moreover, analysis

of other risk factors such as postoperative aortic leaflet height and immediate postoperative echocardiography findings that may potentially affect AR recurrence but were deemed to be beyond the scope of this study were not included since this study aimed to focus on preoperative cardiac CT imaging-related factors. Continuing comprehensive evaluation of multiple clinical and imaging factors over a larger population may yield further valuable information in a future study. Finally, the preference for AV repair over AVR depends considerably on the clinical experience of the cardiac surgeons. Therefore, our results could not be applied in medical institutions that prefer AVR or whose clinicians have less clinical experience.

In conclusion, we evaluated preoperative CT characteristics to predict recurrent AR after the David operation. ARO > 24 mm^2 measured on preoperative CT was an independent factor associated with the development of recurrent AR. Precise evaluation of preoperative CT findings before the operation may be helpful for AR patients who may benefit from the David operation.

Supplementary Materials

The Data Supplement is available with this article at https://doi.org/10.3348/kjr.2019.0446.

ORCID iDs
Hyun Jung Koo
  https://orcid.org/0000-0001-5640-3835
Yura Ahn
  https://orcid.org/0000-0002-9188-1186
Sahmin Lee
  https://orcid.org/0000-0003-2250-7948
Dae-Hee Kim
  https://orcid.org/0000-0002-8275-4871
Jong-Min Song
  https://orcid.org/0000-0002-6754-8199
Duk-Hyun Kang
  https://orcid.org/0000-0003-4031-8649
Jae-Kwan Song
  https://orcid.org/0000-0002-6469-801X
Ho Jin Kim
  https://orcid.org/0000-0002-0809-2240
Joon Bum Kim
  https://orcid.org/0000-0001-5801-2395
Sung-Ho Jung
  https://orcid.org/0000-0002-3699-0312
Suk Jung Choo
  https://orcid.org/0000-0003-4291-302X
Cheol Hyun Chung
  https://orcid.org/0000-0001-8981-6011
Jae Won Lee
  https://orcid.org/0000-0003-0751-2458
Joon-Won Kang
  https://orcid.org/0000-0001-6478-0390
Dong Hyun Yang
  https://orcid.org/0000-0001-5477-558X

REFERENCES

1. Vahanian A, Alfieri O, Andreotti F, Antunes MJ, Barón-Esquivias G, Baumgartner H, et al.; ESC Committee for Practice Guidelines (CPG); Joint Task Force on the Management of Valvular Heart Disease of the European Society of Cardiology (ESC); European Association for Cardio-Thoracic Surgery (EACTS). Guidelines on the management of valvular heart disease (version 2012): the joint task force on the management of valvular heart disease of the European Society of Cardiology (ESC) and the European Association for Cardio-Thoracic Surgery (EACTS). *Eur J Cardiothorac Surg* 2012;42:S1-S44

2. Nishimura RA, Otto CM, Bonow RO, Carabello BA, Erwin JP 3rd, Fleisher LA, et al. 2017 AHA/ACC focused update of the 2014 AHA/ACC guideline for the management of patients with valvular heart disease: a report of the American College of Cardiology/American Heart Association task force on clinical practice guidelines. *J Am Coll Cardiol* 2017;70:252-289

3. Rahimtoola SH. Choice of prosthetic heart valve for adult patients. *J Am Coll Cardiol* 2003;41:893-904

4. Hammermeister K, Sethi GK, Henderson WG, Grover FL, Oprian C, Rahimtoola SH. Outcomes 15 years after valve replacement with a mechanical versus a bioprosthetic valve: final report of the Veterans Affairs randomized trial. *J Am Coll Cardiol* 2000;36:1152-1158

5. Oxenham H, Bloomfield P, Wheatley DJ, Lee RJ, Cunningham J, Prescott RJ, et al. Twenty year comparison of a Bjork-Shiley mechanical heart valve with porcine bioprostheses. *Heart* 2003;89:715-721

6. El Khoury G, de Kerchove L. Principles of aortic valve repair. *J Thorac Cardiovasc Surg* 2013;145(3 Suppl):S26-S29

7. Langer F, Aicher D, Kissinger A, Wendler O, Lausberg H, Fries R, et al. Aortic valve repair using a differentiated surgical strategy. *Circulation* 2004;110(11 Suppl 1):II67-II73

8. Minakata K, Schaff HV, Zehr KJ, Dearani JA, Daly RC, Orszulak

TA, et al. Is repair of aortic valve regurgitation a safe alternative to valve replacement? *J Thorac Cardiovasc Surg* 2004;127:645-653

9. Carr JA, Savage EB. Aortic valve repair for aortic insufficiency in adults: a contemporary review and comparison with replacement techniques. *Eur J Cardiothorac Surg* 2004;25:6-15

10. Aicher D, Fries R, Rodionycheva S, Schmidt K, Langer F, Schäfers HJ. Aortic valve repair leads to a low incidence of valve-related complications. *Eur J Cardiothorac Surg* 2010;37:127-132

11. le Polain de Waroux JB, Pouleur AC, Goffinet C, Vancraeynest D, Van Dyck M, Robert A, et al. Functional anatomy of aortic regurgitation: accuracy, prediction of surgical repairability, and outcome implications of transesophageal echocardiography. *Circulation* 2007;116(11 Suppl):I264-I269

12. Boodhwani M, de Kerchove L, Glineur D, Poncelet A, Rubay J, Astarci P, et al. Repair-oriented classification of aortic insufficiency: impact on surgical techniques and clinical outcomes. *J Thorac Cardiovasc Surg* 2009;137:286-294

13. de Meester C, Pasquet A, Gerber BL, Vancraeynest D, Noirhomme P, El Khoury G, et al. Valve repair improves the outcome of surgery for chronic severe aortic regurgitation: a propensity score analysis. *J Thorac Cardiovasc Surg* 2014;148:1913-1920

14. Koo HJ, Kang JW, Kim JA, Kim JB, Jung SH, Choo SJ, et al. Functional classification of aortic regurgitation using cardiac computed tomography: comparison with surgical inspection. *Int J Cardiovasc Imaging* 2018;34:1295-1303

15. Perry GJ, Helmcke F, Nanda NC, Byard C, Soto B. Evaluation of aortic insufficiency by Doppler color flow mapping. *J Am Coll Cardiol* 1987;9:952-959

16. Lu TL, Huber CH, Rizzo E, Dehmeshki J, von Segesser LK, Qanadli SD. Ascending aorta measurements as assessed by ECG-gated multi-detector computed tomography: a pilot study to establish normative values for transcatheter therapies. E*ur Radiol* 2009;19:664-669

17. David TE. Aortic valve sparing operations: outcomes at 20 years. *Ann Cardiothorac Surg* 2013;2:24-29

18. David TE, Feindel CM. An aortic valve-sparing operation for patients with aortic incompetence and aneurysm of the ascending aorta. *J Thorac Cardiovasc Surg* 1992;103:617-621; discussion 622

19. le Polain de Waroux JB, Pouleur AC, Robert A, Pasquet A, Gerber BL, Noirhomme P, et al. Mechanisms of recurrent aortic regurgitation after aortic valve repair: predictive value of intraoperative transesophageal echocardiography. *JACC Cardiovasc Imaging* 2009;2:931-939

20. Stephens EH, Liang DH, Kvitting JPE, Kari FA, Fischbein MP, Mitchell RS, et al. Incidence and progression of mild aortic regurgitation after Tirone David reimplantation valve-sparing aortic root replacement. *J Thorac Cardiovasc Surg* 2014;147:169-178.e3

21. Yang DH, Kim DH, Handschumacher MD, Levine RA, Kim JB, Sun BJ, et al. In vivo assessment of aortic root geometry in normal controls using 3D analysis of computed tomography. *Eur Heart J Cardiovasc Imaging* 2017;18:780-786

22. Choo SJ, McRae G, Olomon JP, St George G, Davis W, Burleson-Bowles CL, et al. Aortic root geometry: pattern of differences between leaflets and sinuses of Valsalva. *J Heart Valve Dis* 1999;8:407-415

23. Kim DH, Handschumacher MD, Levine RA, Sun BJ, Jang JY, Yang DH, et al. Aortic valve adaptation to aortic root dilatation: insights into the mechanism of functional aortic regurgitation from 3-dimensional cardiac computed tomography. *Circ Cardiovasc Imaging* 2014;7:828-835

24. Di Franco A, Rong LQ, Munjal M, Weinsaft JW, Kim J, Sturla F, et al. Aortic symmetry index: initial validation of a novel preoperative predictor of recurrent aortic insufficiency after valve-sparing aortic root reconstruction. *J Thorac Cardiovasc Surg* 2018;156:1393-1394